BASIC PRINCIPLES OF ANALYTICAL ULTRACENTRIFUGATION

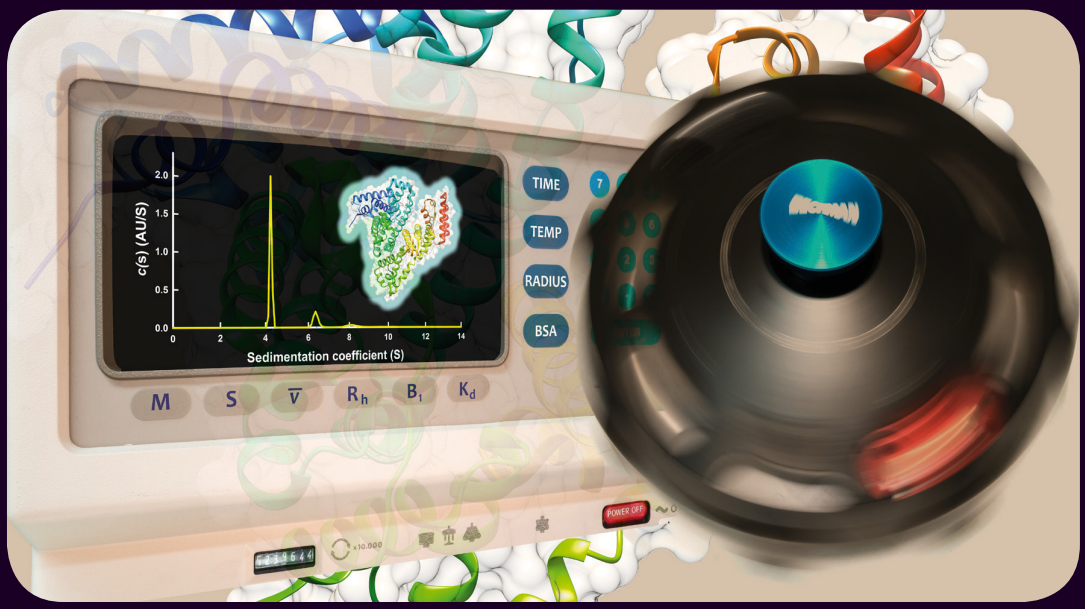

Peter Schuck
Huaying Zhao
Chad A. Brautigam
Rodolfo Ghirlando

CRC Press
Taylor & Francis Group

BASIC PRINCIPLES OF ANALYTICAL ULTRACENTRIFUGATION

This page intentionally left blank

BASIC PRINCIPLES OF ANALYTICAL ULTRACENTRIFUGATION

Peter Schuck
Dynamics of Macromolecular Assembly Section
Laboratory of Cellular Imaging and Macromolecular Biophysics
National Institute of Biomedical Imaging and Bioengineering
National Institutes of Health, Bethesda, Maryland

Huaying Zhao
Dynamics of Macromolecular Assembly Section
Laboratory of Cellular Imaging and Macromolecular Biophysics
National Institute of Biomedical Imaging and Bioengineering
National Institutes of Health, Bethesda, Maryland

Chad A. Brautigam
Department of Biophysics
The University of Texas Southwestern Medical Center
Dallas, Texas

Rodolfo Ghirlando
Laboratory of Molecular Biology
National Institute of Diabetes and Digestive and Kidney Diseases
National Institutes of Health, Bethesda, Maryland

CRC Press
Taylor & Francis Group
Boca Raton London New York

CRC Press is an imprint of the
Taylor & Francis Group, an **informa** business

CRC Press
Taylor & Francis Group
6000 Broken Sound Parkway NW, Suite 300
Boca Raton, FL 33487-2742

Version Date: 20151001

International Standard Book Number-13: 978-1-4987-5116-2 (eBook - PDF)

To T. the Beautiful and L. the Great

Peter Schuck

To my PhD adviser, Dr. Susan Pedigo, who brought me into the biophysical world

Huaying Zhao

To my wife, Lisa, and to all the teachers who have inspired me

Chad A. Brautigam

To Heini Eisenberg who introduced me to the joys of analytical ultracentrifugation

Rodolfo Ghirlando

This page intentionally left blank

Contents

Foreword

This eminently readable book tells the outcome – to present date – of a journey of scientific discovery: A saga in which new territory is explored, peaks conquered, and guideposts left for those who choose to follow. Sedimentation analysis of macromolecular systems is the field in which Dr. Peter Schuck and his fellow investigators have been involved, and to which they have made contributions not only through their own laboratories' investigations, but through the widespread use made of their algorithms and programs by scientists throughout the world. In this present volume we have for our information, guidance (and just plain scientific enjoyment) an up-to-date statement of what an investigator can hope to achieve in the present state of knowledge. Such guidance is most welcome: along with the widespread and worldwide use of the SEDFIT bulletin board and the frequent dedicated training sessions which provide a platform for dissemination of optimal procedures, ideas, findings and opinions.

Scientific knowledge, though, sits in a historical context. The authors here have given credit to 'what has gone before', and to the major volumes which have been published in earlier periods (Svedberg and Pedersen's volume[1] and Schachman's book/monograph[2]). It may be a little unusual today — even 'unfashionable' — to find value in science published more than a decade ago, but for myself I would wish that every would-be young biophysical scientist would read through Cheng and Schachman's remarkable paper (1955 — referenced in this book, and freely available on-line[3]). In this work the authors followed a carefully planned line of enquiry and experimentation to confirm that macromolecular solutes such as proteins could be treated as dispersions of 'hydrodynamic particles' whose properties can be regarded as scale-independent. It speaks volumes for the quality of their experimental work that when they report a study on the concentration-dependence of the sedimentation of polystyrene spheres, they obtain a value for the c-dependence (at high dilution) of the sedimentation rate that comes to within 1% of the best theoretical estimate of this parameter for spheres based upon fluid dynamics, computed decades later (Brady and Durlovsky[4]).

[1] T. Svedberg and K.O. Pedersen, *The Ultracentrifuge*, Oxford University Press, London, 1940.

[2] H.K. Schachman, *Ultracentrifugation in Biochemistry*, Academic Press, New York, 1959.

[3] P.Y. Cheng and H.K. Schachman, Studies on the validity of the Einstein viscosity law and Stokes law of sedimentation, *J. Polym. Sci.*, vol. 16(18), pp. 19–30, 1955, doi:10.1002/pol.1955.120168102.

[4] J.F, Brady and L.J. Durlofsky, The sedimentation rate of disordered suspensions, *Phys. Fluids*, vol. 31(4), pp. 717–727, 1988, doi:10.1063/1.866808.

A particular beauty of sedimentation analysis as a discipline lies in the fact that just a single (differential) equation describes everything. But this 'Lamm' equation cannot be solved directly in the general case. The work of Dr. Schuck and his team is founded upon their demonstration that the fitting by non-linear least squares methods of sets of solutions of the Lamm equation is a stable procedure. Distributions of hydrodynamic parameters, in particular of sedimentation coefficients (s-values), are output. These 'c(s) vs s' distributions have become normative. With many cell scans logged over time the final dataset is highly information-rich, and the time-invariance of most of the noise structure facilitates its effective removal within the software (SEDFIT) environment. By floating other parameters, starting from a solute frictional ratio, within the fit, further information can be yielded as regards solute molecular weight and interaction parameters. Optimal routines are clearly and critically described in this volume.

I will take a moment to recall how great the change is that the use of on-line computation with software sets such as SEDFIT/SEDPHAT has brought to 'prior art'. I began my personal research life in sedimentation analysis working with a Phywe Air-Turbine Analytical Ultracentrifuge, which lacked even rotor temperature control. Data acquisition was achieved using manual scanning of photographic records, and this persisted even into the Beckman Model E era. Computational analysis was with rotary-mechanical calculating machines. Fitting datasets using an 'over-determined set of non-linear simultaneous equations' (*sic*!) was not even a dream of the future. Yet within a decade or two the whole field of sedimentation analysis and indeed of biophysical analysis in general has been transformed by the advent of powerful computational hardware and of equally powerful analytical algorithms and associated software. This growth in activity has provided workers with tools which while simple in concept call for guidance in their use. We in our field have been fortunate indeed to have had over the years scientists of distinction who have been prepared not only to make advances, but to disseminate 'good practice' in application to their colleagues.

Clearly I am talking here with the present authors and their volume in mind; 'c(s) plots computed via SEDFIT' have become the mainstay of a mass of published work, and a foundation for a broader understanding of the nature and properties of macromolecular systems, both in biological and in materials sciences. We have here an authoritative guidance to the wide range of procedures and modes of analysis which are possible. Perhaps I may speculate a little as to how this whole mode of analysis has become so popular?

Excellence is a necessary but not a wholly sufficient explanation for a scientific finding or a new mode of application becoming widely accepted. I suggest that something which I call 'immediate impact' is a necessary part of the package. What do I mean by 'immediate impact'? I will describe what I mean by describing something from my own scientific experience. 'Ostensive definition' is, I believe, the technical term.

Long ago, as part of my extensive involvement with muscle/motility research, I addressed the problem of the basic structure of the myosin thick filament of vertebrate skeletal muscle. A self-assembling structure, interfacing with an ordered

array of thin filaments, it must possess rotational symmetry, to satisfy x-ray and EM structural data. Yet was this a 2-, 3- or 4-fold symmetry? Despite having an ability to prepare purified filaments in low quantity, the apparently simple problem of finding out their mass/unit length gave us an unexpected headache. For reasons which still remain obscure today, the frictional behavior of even 'synthetic filaments' made from pure myosin was found to be seriously anomalous, and depended steeply on the presence of divalent cation, especially of Mg^{++} (Persechini and Rowe, 1984)[5]. We are talking of s-values varying by up to 30%. With Charlie Emes, a graduate student in my lab, an approach was developed which basically accepted the presence of this anomaly, and coped with it, using a neat bit of logic. The answer was simple: 3-fold rotational symmetry it must be. No problems in publishing this finding, in a paper[6] I am very proud of, but it all went over like the proverbial lead balloon. Partly this may have been that the formidable figure of the eminent enzymologist Bill Harrington of Johns Hopkins loomed over our work. Bill was convinced that the symmetry had to be either 2- or 4-fold: All tied up with his view that myosin existed in solution as dimers — the existence of which was denied by both myself[7] and Sara Szuchet[8] of the Yphantis Laboratory. The low-angle x-ray people actually favored 3-fold, but in a heavily qualified manner, so that was not much help.

However, just a couple of years later, another graduate student (Maria Maw) starting work in my lab on the electron microscopy of thick filaments, one day brought to me an image which seemed to show a native thick filament clearly splitting into three sub-filaments. She admitted that she had gotten the preparation procedure for negative staining wrong — she had used a water rinse in place of a solvent rinse. I asked her to do it again just like that, and when she had found and recorded 200 such images I would get seriously excited. She did of course exactly that, and we soon had a paper written and happily grabbed by *Nature*[9] (the only journal of that name in those distant days). That settled the argument. Oh — and for that water rinse, if you take away the charge shielding of a structure held together by charge–charge interactions, it is no great surprise if it starts to fall apart. I did start out my research career as a colloid scientist!

And this is my ostensive definition of immediate impact. If you can show a simple

---

[5]A.J. Persechini and A.J.Rowe, Modulation of myosin filament conformation by physiological levels of divalent cation, *J. Mol. Biol.*, vol.172(1), pp. 23–39, 1984, doi:10.1016/0022-2836(84)90412-1.

[6]C.H. Emes and A.J. Rowe, Frictional properties and molecular weights of native and synthetic myosin filaments from vertebrate skeletal muscle, *Biochim. Biophys. Acta*, vol. 537(1), pp.125–144,1978, doi:10.1016/0005-2795(78)90608-6.

[7]C.H. Emes and A.J. Rowe. Hydrodynamic studies on the self-association of vertebrate skeletal muscle myosin, *Biochim. Biophys. Acta*, vol 537(1), pp. 110-124, 1978, doi:10.1016/0005-2795(78)90607-4.

[8]S. Szuchet, Effect of purification procedures on the self-association of myosin at high ionic strength, *Arch. Biochem. Biophys.*, vol. 180(2), pp. 493–503, 1977, doi:10.1016/0003-9861(77)90064-9.

[9]M.C. Maw and A.J. Rowe, Fraying of A-filaments into three subfilaments, *Nature*, vol. 286(5771), pp. 412–414, 1980, doi:10.1038/286412a0.

image or convincing graph of what you are talking about then a few equations and sound interpretations are not the whole thing in the game. Quality of analysis and interpretation has to be a starting point. But output which makes an immediate impact is the vital, last stage in any fruitful investigation. The work of the four scientists who have authored this volume excel in all of this, and this book will be as vital a tool for novices as much as for senior workers seeking guidance on the more recondite areas of analysis.

And for the future, where may we be heading? There are trends already established for the increasing level of study of non-biological systems (polymers), and for the use of the AUC within the bio/pharma industry. The acceptance of c(s) profiles as a matrix-free 'gold standard' method orthogonal to column-based technology has undoubtedly encouraged interest and commitment within the bio/pharma sector, and we can expect that area of activity to increase. I am also certain that the present achievement levels of the AUC hardware/software can be surpassed. The instrument provides data at a remarkably high level of precision, particularly when Rayleigh interference optics are being employed. The ultimate level of random 'shot noise', shown to be ± 0.002 fringe, can probably not be surpassed, even in a newly designed optical system: But when the total signal is usually in the range 1–300 fringe, the theoretically available precision (signal/noise ratio) leaves many biophysical analytical instruments well behind. Most ways of probing systems in solution involve the pertubation of basic physical parameters of the system: exposure to magnetic fields, temperature jumps, particle–photon interactions, for example. A pertubation of a centrifugal field ('g-force') is so simple and basic an approach that there should always be a place for its employment. The authors of this book have given us, not a compendium, but a monograph based upon their extensive experience in the field of sedimentation analysis — which incidentally they have been at pains to relate to results from other biophysical techniques, such as dynamic light scattering. Readers and potential readers: If you already know about sedimentation analysis you will find interest and information alike in its pages. If you are a newcomer to the area, you should take advantage of the opportunity to read a well-written and authoritative account, and become excited by its possibilities.

Arthur J. Rowe, Nottingham University, U.K.

Preface

Analytical ultracentrifugation (AUC) consists of the application of a high gravitational field to a solution of particles and the real-time detection of the evolving spatial concentration gradients. When applied to macromolecules or nanoscopic particles, ultracentrifugation data can provide rich information on their shape, solvation, composition and size-distribution, as well as allow for a detailed view of their reversible single- or multi-component interactions over a wide range of affinities. After almost a century of methodological development, stimulated by ever-changing emphasis in applications, as well as substantial instrumental and computational advancements, a wealth of theoretical and experimental knowledge of sedimentation has been accumulated. Unfortunately, no systematic textbook or comprehensive monograph on AUC has been published since the initial work by Svedberg and Pedersen 1940, and the seminal detailed methodological summary by Schachman, 1959. This has rendered AUC a discipline that is hard to master without direct access to experienced laboratories where it is routinely practiced, and hampers this powerful technique from once again becoming a mainstream tool in the molecular sciences.

The goal of the present book is to provide a description of the basic principles in theory and practice, sufficiently comprehensive for the reader to confidently practice AUC, and to be aware of its full potential and possible pitfalls. The book aims to help the reader gain a solid understanding of the basic concepts, and to facilitate further reading of the referenced detailed topics, with appreciation for their historic and current relevance. The emphasis is experimental, and more detailed descriptions of the theoretical frameworks and data analysis strategies are planned in forthcoming volumes. Although we always strived to provide the most important and historically accurate references, we recognize that ambiguities exist, and apologize for any perceived omissions or limitations in our knowledge.

The first chapter introduces the basic principles and technical setup of an analytical ultracentrifugation experiment, together with a brief description of the optical systems used for detection. The ultracentrifugation experiment is subsequently explored in Chapter 2 from a macromolecular standpoint to arrive at a detailed physical picture of the sedimentation process, from which to derive the relevant macromolecular parameters. Next, we recapitulate important practical aspects for conducting an experiment, including sample preparation (Chapter 3), details on data acquisition and data structure (Chapter 4), and the practical execution of the centrifugal experiment (Chapter 5). Instrument calibration and quality control experiments are outlined in Chapter 6. Tables of often useful data for AUC,

including the properties of common macromolecules and solvents, are assembled in the appendices.

Throughout, to enrich the utility of the book and illustrate the facility of practical application of ideas ranging from simple to advanced, specially marked textboxes highlight how the topic at hand corresponds to AUC-related functions in the widely used data analysis programs `SEDFIT` and `SEDPHAT`, which can be freely obtained from the website of the Dynamics of Macromolecular Assembly Section of the National Institute of Biomedical Imaging and Bioengineering at sedfitsedphat.nibib.nih.gov. Although the book is conceived as a standalone reference, it also provides a broader background to our workshops on AUC and related biophysical techniques at the National Institutes of Health.

We hope this book fills a gap in the literature of biophysical methodology, and will offer the reader interesting and useful material.

Peter Schuck
Huaying Zhao
Chad A. Brautigam
Rodolfo Ghirlando

This work was supported by the Intramural Research Programs of the National Institute of Biomedical Imaging and Bioengineering, and the National Institute of Diabetes and Digestive and Kidney Diseases at the National Institutes of Health.

SYMBOL DESCRIPTION

$_1$	index 1 to denote solvent component in multi-component mixtures
a	chemical activity
$_a$	subscript 'a' to indicate the macromolecular component
$A(r)$	radial dependence of the absorbance
$a\,(r,t)$	radial- and time-dependent signal
$a^*\,(r,t)$	radial- and time-dependent signal after consideration of various optical detection effects
β	in the context of nonlinear detection, the nonlinearity exponent
$\beta(t,\omega)$	time- and/or rotor-speed dependent baseline signal offset that is radially constant ('RI noise')
b	bottom radius (distance from center of rotation to the distal end of the solution column)
$b(r)$	radial-dependent baseline signal offset that is temporally constant ('TI noise')
B_1	preferential binding parameter for water
B_3	preferential binding parameter for co-solute
c	molar concentration
$c(s)$	diffusion-deconvoluted differential sedimentation coefficient distribution
$c_B^*(c_A)$	phase transition line (in concentration of the larger component B) of the vanishing undisturbed boundary in the effective particle model
χ^2	measure for fit quality
$\delta_{i,j}$	Kronecker symbol, $\delta_{i,j} = 1$ if $i = j$, else $\delta_{i,j} = 0$
δ_{beam}	effective beam diameter in the fluorescence detector
$\delta(r,t)$	the statistical noise of each data point at radius r and time t
Δl	optical pathlength difference
ΔJ	fringe displacement
D	diffusion coefficient
D_{norm}	normalized volume of spectra basis in MSSV
dn/dw	refractive index increment based on weight-concentration (in the literature often referred to as dn/dc)
ε	molar extinction coefficient
$\varepsilon_{\mathrm{molar}}$	molar extinction coefficient
$\varepsilon^{(IF)}$	molar effective fringe increment
$d\varepsilon/dr$	spatial gradient of specific signal increment in fluorescence detection
η	solvent viscosity
η_0	standard viscosity (of water at 20°C in 1 atm)
f	hydrodynamic translational friction coefficient
f_0	translational friction coefficient of the equivalent compact, smooth sphere with same mass and density as the particle
F_b	buoyancy force
F_f	frictional force
F_{sed}	sedimentation force
$\phi(r,s)$	radial- and s-value dependence of the incident photon flux in FDS detection
γ	chemical activity coefficient
$I(r)$	radial dependence of the transmitted light intensity in the sample sector
$I_0(r)$	radial dependence of the transmitted light intensity in the reference sector
j_{sed}	sedimentation flux
j_{diff}	diffusion flux
k	in density contrast experiments with heavy water, the relative

	increase in mass due to H-D exchange
κ	solvent compressibility coefficient
k_B	Boltzmann constant
K	association equilibrium constant
K_β	nonlinearity constant
K_D	dissociation equilibrium constant
k_{off}	chemical off-rate constant
k_s	non-ideality coefficient of sedimentation
k_D	non-ideality coefficient of diffusion
λ	wavelength
l	optical pathlength
μ	chemical potential
m	meniscus radius (distance from the center of rotation to the proximal end of the solution column)
m_a	mass of particle
M	molar mass
M_a	molar mass of the macromolecular component
M_b	buoyant molar mass
$M_{app,b}$	apparent buoyant molar mass
$M_{b,PD}$	buoyant molar mass in the 'play dough' formalism
M_{PD}	molar mass in the 'play dough' formalism of an unhydrated object of certain shape and density
M_{PZ}	molar mass of a polymeric macroion P jointly with z monovalent counterions
M_S	molar mass of a mono-valent salt
M_1	mass of bound water per mol of protein
ω	rotor angular velocity
ϕ'	effective partial specific volume
Π	osmotic pressure
$p(r)$	radial distribution of the pressure in the solution column
$^{(p)}$	superscript to denote a non-diffusing particle
$_{PD}$	subscript to denote a quantity in the 'play dough' formalism of a solid, unhydrated, inert object of uniform density
ρ	solvent density
ρ_0	standard density (of water at 20 °C in 1 atm)
r	radius (distance from the center of rotation)
r_0	reference radius (arbitrarily chosen)
r_{DH}	in density contrast experiments with heavy water, the molar ratio of D to (H + D)
R	gas constant
R^*	in density contrast experiments, the ratio of buoyant molar masses or viscosity corrected sedimentation coefficients
R_0	radius of the equivalent compact, smooth sphere with same mass and density as the particle
R_S	Stokes radius
$r.h.s.$	right-hand side (of an equation)
rms	root mean square
$rmsd$	root mean square deviation
s	sedimentation coefficient
s_0	ideal sedimentation coefficient in the limit of infinite dilution
$s_{A\cdots B}$	sedimentation coefficient of the reaction boundary in a rapidly interacting system, as denoted in the framework of the effective particle model
$s(r,t)$	spatio-temporal evolution of signal
s_w	signal weighted average sedimentation coefficient
$s_{20,w}$	sedimentation coefficient corrected to standard conditions
$_{SP}$	subscript to denote a quantity in the 'sedimenting particle' formalism
t	time (but in appendix B referring to the temperature in °C)

$t^{(sed)}$	effective sedimentation time	v	particle absolute velocity
T	absolute temperature	v_{scan}	velocity of the scanner
$\bar{v}$	partial-specific volume	w	weight concentration
$\bar{v}_a$	partial-specific volume of the macromolecular component	w_a	weight concentration of a macromolecule 'a'
$\bar{v}_{PD}$	partial-specific volume in the 'play dough' formalism	ξ	preferential binding parameter
$\bar{v}_{SP}$	partial-specific volume in the 'sedimenting particle' formalism	$_{xp}$	subscript to denote 'experimental'
$\bar{v}_1$	partial-specific volume of bound water	z	number of charges (in different context, also denoting end-to-end distance of worm-like chain)

This page intentionally left blank

Analytical Ultracentrifugation Basics

THE GOAL of this first chapter is to provide an initial overview of the basic experimental setup in analytical ultracentrifugation (AUC), a consideration of the forces involved and a first introduction of the fundamental equations. This will be linked with a brief description of the optical detection systems to set the stage for more detailed considerations in the subsequent chapters.

1.1 PHYSICAL PRINCIPLES

An analytical ultracentrifuge consists of an optical detection system integrated into an ultracentrifuge, allowing for the real-time detection of the evolution of the concentration distribution of particles subjected to centrifugation. Two major experimental methods are employed in analytical ultracentrifugation, which differ in the applied centrifugal force: sedimentation velocity (SV) and sedimentation equilibrium (SE). Many excellent reviews and monographs have been written during the long history of this technique (among them, [1–8]), and in the following we only recapitulate the basic principles.

1.1.1 Basic Experimental Setup

Analytical ultracentrifugation was pioneered in the early 20th century by Theodor (The) Svedberg[1] [9, 14, 15]. Prior to that, principles of sedimentation equilibrium in solution had been discovered by Jean Perrin [16, 17], but experiments had been

[1]Theodor (The) Svedberg developed the oil-turbine ultracentrifuge for the study of concentration gradients of dissolved particles, and received the Nobel Prize in Chemistry 1926 "for his work on disperse systems" [9]. For a scientific biography see [10]. Other significant contributors in the technical development of analytical ultracentrifuges were Jesse Wakefield Beams and Edward Greydon Pickels, who developed air-turbine ultracentrifuges [11], initially for different purposes, and later ultracentrifuges with electrical drives. The electrical drives were widely adopted, and ultimately led to the widespread use of analytical and preparative ultracentrifuges. For a detailed historical account of the development of the analytical ultracentrifuge, see the work of Boelie Elzen [12, 13].

confined to large particles for which analytical sedimentation in the earth's gravitational field (∼1 g) was sufficient. In the analytical ultracentrifuge, the choice of rotor speed provides a convenient opportunity to scale the magnitude of the gravitational field from 100 g to 300,000 g, corresponding to rotor speeds of 1,000 and 60,000 rpm with current analytical rotors. This flexibility permits the study of particles over a large size-range, spanning molar masses from 100 Da up to 1 GDa.[2]

The implementation of AUC is conceptually very simple. The rotor spins in an evacuated, temperature-controlled chamber[3] that isolates the sample solution and suppresses temperature-driven convective flows. The sample is loaded in a cell assembly placed in the rotor such that it is sandwiched between quartz or sapphire windows that are transparent to the optical detection system. The detection system probes the concentration distribution of the sample solution in a radial direction, with light traveling through the sample in a direction parallel to the axis of rotation.

All but the earliest analytical ultracentrifuges share the basic design depicted in Fig. 1.1. Usually, the centrifugal cell contains a centerpiece with two sector-shaped solution columns, one for the sample and the other for the matching solvent buffer used as an optical reference. Most of the current detection systems are mounted within the evacuated rotor chamber, although sometimes light is guided out of the chamber for detection such as in the case of the Spinco Model E and Svedberg's original instrument.

1.1.2 Sedimentation Velocity

An SV experiment is basically the observation of the free fall of particles in solution under the influence of a strong gravitational field: in the reference frame of the spinning solution column, the centrifugal force is equivalent to a gravitational force.[4] This force is proportional to the square of the rotor speed $F_{\text{sed}} = m_a\omega^2 r$, where m_a is the particle mass, ω the rotor angular velocity, and r the distance from the center of rotation. During sedimentation, the macromolecules are subject to buoyancy forces that oppose the gravitational force. Based on Archimedes' principle, the magnitude of the buoyancy force is equal to the gravitational force on the displaced solvent. Sedimentation, neutral buoyancy, or flotation may be observed, depending on the relative densities of the immersed particle and solvent. Even though this adds a level of complexity to the sedimentation experiment, this property can be exploited to study the particle density or composition via contrast variation, in a manner analogous to scattering techniques [20]. Thus, the particle partial-specific

[2]We will be expressing molar masses in Daltons (Da), as equivalent to 1 g/mol. Likewise, when expressing the absorbance of solutions we will use OD units interchangeably with AU.

[3]The vacuum system of the ultracentrifuge was developed by Beams and Pickels in the 1930s and 1940s [12, 18]. It allows for a reduction in friction heat generated at high speeds and thereby enables the maintenance of constant temperature.

[4]Under usual experimental conditions, both the earth's gravitational field and the Coriolis force are negligible [19].

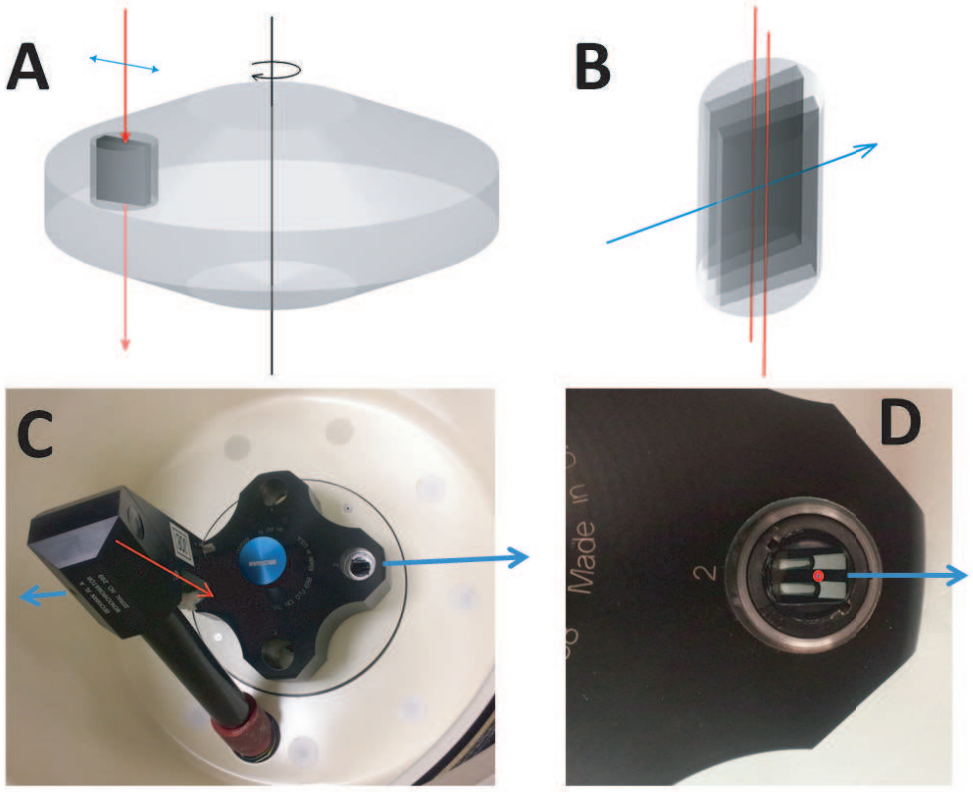

Figure 1.1 Geometry of analytical ultracentrifugation. *Panel A*: Schematics of an analytical ultracentrifugation rotor, with a sector-shaped sample volume (dark gray) in a cylindrical sample cell, and the light path in the optical system (red arrow), which is triggered with the revolution of the rotor (black curved arrow), scanning the concentration distribution in radial direction (blue double sided arrow). *Panel B*: Schematic side view of a double sector cell assembly, with two liquid solution columns (often one used as a sample and one as optical reference) and light paths of optical detection (red lines), with the direction of the gravitational field indicated by the blue arrow. *Panel C*: Picture of a 4-hole An-60 Ti rotor inside the chamber of an analytical Optima XL-A ultracentrifuge (Beckman Coulter), with the attachment for the absorbance optics installed. *Panel D*: Top view of the sample cell inside the rotor (with the red dot indicating a viewpoint along the direction of the red arrow in Panel A). It contains ∼200 μL of an aqueous sample in a 12 mm centerpiece, with the meniscus in both sample and reference compartment visible approximately at half height.

volume, $\bar{v}$, and the solvent density, ρ, become relevant quantities in the buoyancy force $F_b = -m_a\bar{v}\rho\omega^2 r$, with $m_a\bar{v}\rho$ representing the mass of solvent displaced. As noted later (Section 2.1), a determination of what should be considered the volume of the sedimenting particle is not trivial, as this can include contributions from hydration, weakly bound co-solutes, and locally altered solvent, among others.

The sum of the centrifugal and buoyancy forces is matched by a frictional force, which arises from the hydrodynamic translation of the particle migrating in solution (Fig. 1.2). It is due to the work required to move solvent molecules to create space for the sedimenting particle and to move the solvent molecules in the zone of hydrodynamic drag. The frictional force is opposed to migration, and its magnitude is proportional to the absolute velocity of migration v, taking the form $F_f = -vf$, where f represents the hydrodynamic translational friction coefficient.[5]

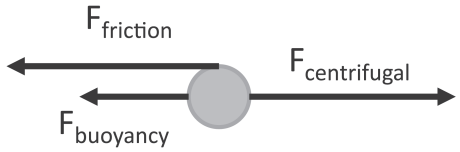

Figure 1.2 Frictional, centrifugal, and buoyancy forces acting on a particle during SV.

It is more convenient to express the sedimentation velocity in terms that reflect the particle's molecular properties, independent of the applied gravitational field, $\omega^2 r$. This is accomplished by normalizing the particle's velocity relative to the gravitational field, thus defining the sedimentation coefficient:

$$s = \frac{v}{\omega^2 r} \tag{1.1}$$

It is measured in units of Svedberg, abbreviated S, with 1 S = 10^{-13} sec. Following custom, the sedimentation coefficient will also be alternately referred to as the 's-value'. The sign of the s-value can be positive or negative, dependent on the relative densities of the particle and solvent resulting in either sedimentation (positive sign) or flotation (negative sign). The balance of forces leads to a relationship of s in terms of the molecular mass and friction:

$$s = \frac{m_a\,(1 - \bar{v}\rho)}{f} \tag{1.2}$$

[5] As an example for the magnitude of the frictional force, a BSA monomer with a s-value of ~4.3 S will sediment with a velocity of ~0.8 μm/sec at 50,000 rpm and experience a frictional force of ~0.05 fN.

SEDFIT – In the Options ▷ Calculator menu, the frictional force can be calculated for a sedimenting particle under given experimental conditions.

We can express the frictional coefficient using Stokes' law and the Stokes radius R_S as

$$f = 6\pi\eta R_S \tag{1.3}$$

where η is the solvent viscosity and R_S is the radius of an equivalent sphere that has the same frictional coefficient as the particle under consideration (but not necessarily the same mass).[6,7] R_S can be expressed relative to the radius R_0 of a hypothetical solid and smooth spherical particle that has the same mass and density as our sedimenting particle. We may imagine a solvent free, compact particle composed of play dough modeling material;[8] which when compacted into a solid sphere would have a radius R_0, and corresponding translational friction coefficient f_0. The frictional ratio $f/f_0 = R_S/R_0$ describes the excess friction our original particle exhibits relative to that sphere arising from rearranging its mass in the most compact form. The value of f/f_0 is frequently utilized as a measure of shape asymmetry, but it should be noted that values > 1.0 do not necessarily imply asymmetric particle contours.[9] Together with Eq. (1.2), this leads to the following relationship for the sedimentation coefficient:

$$s = \frac{m_a\,(1 - \bar{v}\rho)}{6\pi\eta R_0\,(f/f_0\,)} \tag{1.4}$$

Accordingly, aside from the dependence on solvent density and viscosity, s is a molecular constant, reporting on the molecular mass, partial-specific volume, and shape. To remove the dependence on the solvent properties, it is customary to convert the experimental s-values to values that would be observed if the experiment were carried out in water at 20 °C having a density ρ_0 of 0.9982 g/mL and a viscosity η_0 of 1.002×10^{-3} Pa·sec (or 0.01002 Poise). This now allows a comparison of s-values

[6]Cheng and Schachman [21] have experimentally confirmed that the Stokes' law of sedimentation and Einstein law of viscosity indeed hold for microscopic particles, although derived on the assumption that particles are large relative to the molecules of the solvent medium.

[7]This holds true for stick boundary conditions. In organic solvents slip boundary conditions apply, and the frictional coefficient becomes $f = 4\pi\eta R_S$.

[8]We envisage a malleable material of constant density and well defined surface that can be of different shape, but at constant mass and uniform density.

[9]For example, we can imagine a ball of play dough of radius r_0 was formed into a particle with a hollow spherical shell of outer radius $r_1 = 2r_0$; it would be round but have a frictional ratio 2.0. Also, the value of the frictional ratio is dependent on the definition of the sedimenting particle (see Chapter 2) and whether, for example, solvation is included. Customarily, hydration is not included, such that tightly bound water will appear to create additional macromolecular 'shape asymmetry' when determined using f/f_0. Typical values for proteins range from 1.2 to 1.5 for shapes that are globular to moderately elongated [22, 23], but can be as small as 1.1 for some γ-crystallins with compact shape and low hydration [24, 25].

determined in different buffers and temperatures. Using these standard conditions, $s_{20,w}$ is defined:

$$s_{20,w} = s_{xp} \frac{\eta_{xp}}{\eta_0} \frac{(1 - \bar{v}_0 \rho_0)}{(1 - \bar{v}_{xp} \rho_{xp})} \tag{1.5}$$

(with the subscript 'xp' indicating the experimental values).[10]

SEDFIT – A function in the Options ▷ Calculator menu transforms experimental s-values to $s_{20,w}$-values. For a complete sedimentation coefficient distribution, provided that all species visible have the same $\bar{v}$, this transformation can be done in the Options ▷ Size Distribution Options menu.

An example for the s-values as a function of particle mass and shape for proteins with a range of frictional ratios in aqueous solutions is given in Fig. 1.3.

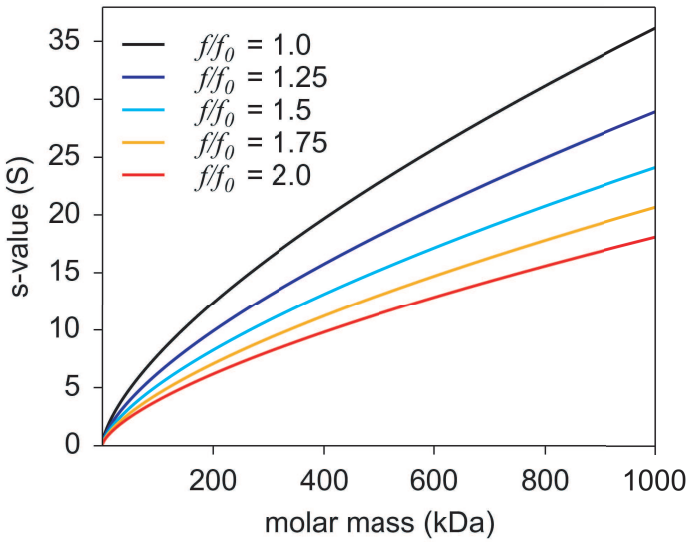

Figure 1.3 Dependence of the approximate s-value of proteins in aqueous solvents on the protein molar mass and frictional ratio, approximated as $s_{20,w} \approx 0.012 M^{2/3} \ (1 - \bar{v}\rho) \, \bar{v}^{-1/3} \ (f/f_0 \ )^{-1}$ with s in units of S, M in Dalton, $\bar{v}$ in mL/g (assumed here to be 0.73 mL/g) and ρ in g/mL (assumed here to be the standard density of 0.9982 g/mL). Shown is a family of curves with different f/f_0 values. The black curve with $f/f_0 = 1.0$ represents the fastest possible sedimentation velocity for a particle of the given mass and density. Frictional ratios in excess of 2.0 are rare (but not impossible) for folded proteins, but higher values will occur for worm-like chains or rod-like particles, such as nucleic acids and chromatin arrays.

[10]Note this relationship is incorrect in ref. [26].

SEDFIT – In the Options ▷ Calculator menu a function is available to predict the s-value as a function of frictional ratio, partial-specific volume, buffer density, and buffer viscosity.

In the simplest depiction of sedimentation, we can calculate the trajectory of a single, non-diffusing particle, $r^{(p)}(t)$, by using the definition of the s-value Eq. (1.1) to determine the position-dependent velocity, which leads to a differential equation:

$$\frac{dr^{(p)}}{dt} = s\omega^2 r^{(p)} \tag{1.6}$$

It has the solution:

$$r^{(p)}(t) = r_0 e^{s\omega^2 t}$$

$$r^{(p)}(t) = m e^{s\omega^2 t} \tag{1.7}$$

where r_0 is the particle position at $t = 0$. With the starting position taken as the meniscus position m, Eq. (1.7) may be used to describe the propagation of a sedimentation boundary of non-diffusing species. Since the centrifugal field increases with radius, it produces an acceleration that increases with time, such that particles are expelled exponentially from the center of rotation (Fig. 1.4).[11]

This simple, single-particle model omits environmental forces that act on the particle, such as those responsible for diffusion, as well as forces arising from the presence of other macromolecules. The latter include long-range electrostatic forces, steric repulsion under high macromolecular concentrations, or short-range attractive forces leading to transient complex formation. Their influence and analysis are frequently of great importance and their treatment will be the topic of Section 2.2.

However, it is possible at this stage to relate the process of sedimentation to diffusion via the common assumption that both share the same translational friction coefficient (for limitations of this assumption, see e.g. Section 2.3). In such a case, the Stokes–Einstein relationship $D = k_B T/(6\pi\eta R_S)$ (with k_B the Boltzmann constant and T the absolute temperature) can be used, jointly with Eq. (1.2) to arrive at the Svedberg equation [27]:

$$\frac{s}{D} = \frac{M\,(1 - \bar{v}\rho)}{RT} \tag{1.8}$$

where M denotes the particle molar mass, and R is the gas constant. The Svedberg equation is very important in that it relates the three most fundamental quantities that can be measured directly in sedimentation experiments: the sedimentation coefficient (obtained from the migration of the sedimentation boundary with time

[11] In the case of flotation, characterized by a negative sedimentation coefficient s due to particle densities lower than the solvent density, Eq. (1.7) describes the particle migrating toward the center of rotation with a decreasing absolute velocity.

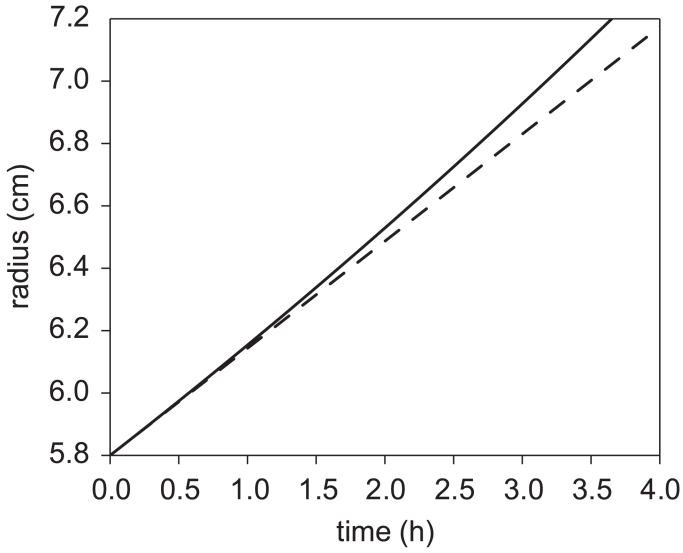

Figure 1.4 Radial position as a function of time for a 6 S species sedimenting at 50,000 rpm, starting at a position at 5.8 cm and following Eq. (1.7) (solid line). For comparison, the trajectory that would correspond to a constant velocity is shown as a dashed line. Over the radial range covered within the geometric constraints of the current analytical ultracentrifuge, the exponential acceleration is qualitatively not large, but nonetheless significant for all quantitative considerations.

in SV), the diffusion coefficient (obtained from the spread of the sedimentation boundary with time), and the molar mass (obtained from the exponential gradient in SE, see below).

`SEDFIT` – Even though the default description of macromolecular sedimentation and diffusion in the discrete non-interacting species model is phrased in terms of molar mass and sedimentation coefficient, from which the diffusion coefficients are calculated via the Svedberg equation (1.8) the `Options ▷ Fitting Options ▷ Fit M and s` function can toggle the program into a mode where the diffusion coefficient can be directly entered, and molar masses are then calculated implicitly in conjunction with the given sedimentation coefficient. Similarly, a switch of coordinates from diffusion coefficients into Stokes radii is possible when analyzing dynamic light scattering data, using the function `Model ▷ Dynamic Light Scattering ▷ Discrete Stokes Radii`.

For large macromolecules, macromolecular assemblies and many nanoparticles with R_0 greater than 10–15 nm, SV experiments are usually conducted under conditions such that the root-mean-square (r.m.s.) distance particles travel by diffusion is small or even negligible compared to the migration by sedimentation. However, for most macromolecules, the opposite is true under typical experimental conditions. Therefore, in revising the analyses presented in Fig. 1.2 and Fig. 1.4, it is more accurate to imagine an ensemble of molecules where the individual molecules mostly

undergo a random walk from diffusion, which is biased by the centrifugal field. This is schematically depicted in Panel A of Fig. 1.5 but can be better visualized in a movie simulating biased random walk [28].[12]

We can now anticipate the main features of a real SV experiment, in which we study a large ensemble of particles,[13] and monitor their concentration as a function of time and radial distance [28]. In such an experiment, a sector-shaped solution column usually starts out with a uniform distribution of particles. In the frame of reference of the spinning solution column, we will refer to the direction of the centrifugal force as 'down' and its distal end as the 'bottom' (at radius b) of the centrifugal cell. At the upper end of the solution column is the meniscus (at radius m), representing the air-solution interface. The solution column in SV typically includes radial distances of ∼6.0 cm to ∼7.2 cm from the center of rotation.

When centrifugation starts, all molecules sediment at a velocity $v = s\omega^2 r$ that is dependent on their radial position, where they experience the exponential acceleration described above. Will the ensuing radial differences in velocity create a concentration gradient? To answer this, let us observe a volume element ΔV between radius r_1 and $r_2 = r_1 + \Delta r$, of a height h, and with an average width in the plane of rotation of $\bar{y} = \varphi\bar{r}$ (with φ the angle of the sector-shaped solution column, usually 2.4°, and the average radius $\bar{r} = r_1 + \Delta r/2$). This is depicted in Panel B of Fig. 1.5. Following a small increment of time dt, the radial boundaries of this volume element will have migrated to ${r_1}' = r_1 + s\omega^2 r_1 dt$ and ${r_2}' = r_2 + s\omega^2 r_2 dt$, i.e., to radii larger by a factor $\left(1 + s\omega^2 dt\right)$. The height stays unchanged, but the width has grown to $\bar{y}' = \varphi\left(\bar{r} + s\omega^2\bar{r}dt\right)$, namely by the same factor $\left(1 + s\omega^2 dt\right)$. The volume element $\Delta V = (r_2 - r_1)h\bar{y}$ will still contain the same number of molecules, but based on the change in width and radii of the boundaries, the volume element will increase by a factor $\Delta V'/\Delta V = (1 + s\omega^2 dt)^2$, which is the square of the radial displacement factor. Importantly, the magnitude of this dilution during the sedimentation process is independent of radius, and will therefore not result in a radial concentration gradient. Furthermore, due to the sector-shaped solution column and the radial acceleration experienced by the migrating particles, the particle concentration will decrease over time,[14] such that:

$$\frac{c(t')}{c(t)} = \left(\frac{r(t)}{r(t')}\right)^2 \tag{1.9}$$

[12]From a set of experimental scans obtained during the sedimentation of a monodisperse single species, a comparison of the r.m.s. displacement by diffusion and sedimentation can be made from the width of the sedimentation boundary relative to its distance from the meniscus, see below.

[13]A typical sample for SV, 0.4 mL of a 1 μM solution, will contain ∼2.4×10^{14} macromolecules.

[14]More quantitatively, the relative change in concentration will be proportional to the increase in the size of the volume element $(dc/dt\,)/c = -(d\Delta V'/dt\,)/\Delta V$. After dropping quadratic terms, we find $(dc/dt\,)/c = -2s\omega^2$, from which $c(t) = c(t_0)e^{-2s\omega^2(t-t_0)}$ follows. This is a special case solution of the Lamm equation (Eq. 1.10 below) for the plateau region, i.e., in the absence of diffusion.